SCIENTIFIC REPORTS

OPEN

SUBJECT AREAS:
COMPUTATIONAL CHEMISTRY
QUANTUM CHEMISTRY
MOLECULAR DYNAMICS
METAL COMPLEXES

Received
4 November 2013

Accepted
2 January 2014

Published
23 January 2014

Correspondence and requests for materials should be addressed to M.Z.A. (mzan@hit.edu.cn)

A Combined Theoretical and Experimental Study for Silver Electroplating

Anmin Liu, Xuefeng Ren, Maozhong An, Jinqiu Zhang, Peixia Yang, Bo Wang, Yongming Zhu & Chong Wang

State Key Laboratory of Urban Water Resource and Environment, School of Chemical Engineering and Technology, Harbin Institute of Technology, Harbin, 150001, People's Republic of China.

A novel method combined theoretical and experimental study for environmental friendly silver electroplating was introduced. Quantum chemical calculations and molecular dynamic (MD) simulations were employed for predicting the behaviour and function of the complexing agents. Electronic properties, orbital information, and single point energies of the 5,5-dimethylhydantoin (DMH), nicotinic acid (NA), as well as their silver(I)-complexes were provided by quantum chemical calculations based on density functional theory (DFT). Adsorption behaviors of the agents on copper and silver surfaces were investigated using MD simulations. Basing on the data of quantum chemical calculations and MD simulations, we believed that DMH and NA could be the promising complexing agents for silver electroplating. The experimental results, including of electrochemical measurement and silver electroplating, further confirmed the above prediction. This efficient and versatile method thus opens a new window to study or design complexing agents for generalized metal electroplating and will vigorously promote the level of this research region.

Silver is widely used in microelectronics, aerospace, automotive, and jewelries due to its excellent physiochemical properties, good corrosion resistance, high bulk conductivity, and beautiful features for decorative purposes[1].

During more than 100 years application, the mirror bright, compact, smooth, and adhesive silver deposits were usually realized from cyanide baths, which offer the most consistent deposit qualities at the lowest cost[2–6]. Unfortunately, cyanide is one of the most toxic chemicals, which brings extremely high risks to human health and the environment, especially when operated these cyanide-based baths at a high temperature[7].

To solve this problem, a number of attempts have been made in past few years to develop cyanide-free silver plating baths. Among them, the complexing agents for silver electroplating were widely investigated owing to its important roles during the electroplating process. In conclusion, complexing agents for cyanide-free silver plating baths, such as thiosulfate[8,9], hydantoin[10,11], 5,5-dimethylhydantoin[12], uracil[13], succinimide[14,15], sulfite[16], ammonia[17–19], thiourea[20,21], HEDTA[22], 2-hydroxypyridine[23,24], and ionic liquids (ILs)[25–28], *etc.* have been proposed.

Considering the satisfactory bath and deposit performances, it is necessary to design a plating bath with excellent consistent deposit quality and reliability. Generally, these attempts were intensively studied by experiments. Some complexing agents for cyanide-free silver electroplating were found recently after enormous experiments. However, except for few successful cases, most of the results were unsatisfied. The silver plating baths still suffer from problems of unstable, light, high cost, sensitive to temperature, relatively high toxicity, and sometimes the silver ions are eventually reduced to the metal with low quality deposits in terms of adhesion and morphologies, *etc*. Therefore, a more effective approach should be explored to choose or design the desired cyanide-free silver plating baths.

In the last decades, quantum chemistry, computational chemistry and molecular modeling were fast emerging for the calculation, modeling and simulation of small chemical and biological systems, in order to understand and predict their behaviors at the molecular level[29–34]. Quantum chemical calculations and molecular dynamic simulations have become useful methods to study many natural systems in pharmacology, chemistry, and biology.

Density functional theory (DFT) has made an unparalleled impact on the application of quantum mechanics to interesting and challenging problems in chemistry for the past decades[30,31,35–43], which allows us to compute all properties of systems by the electron density $\rho(r)$ as a function of three variables: $\rho(r) = f(x, y, z)$. As it confirmed,

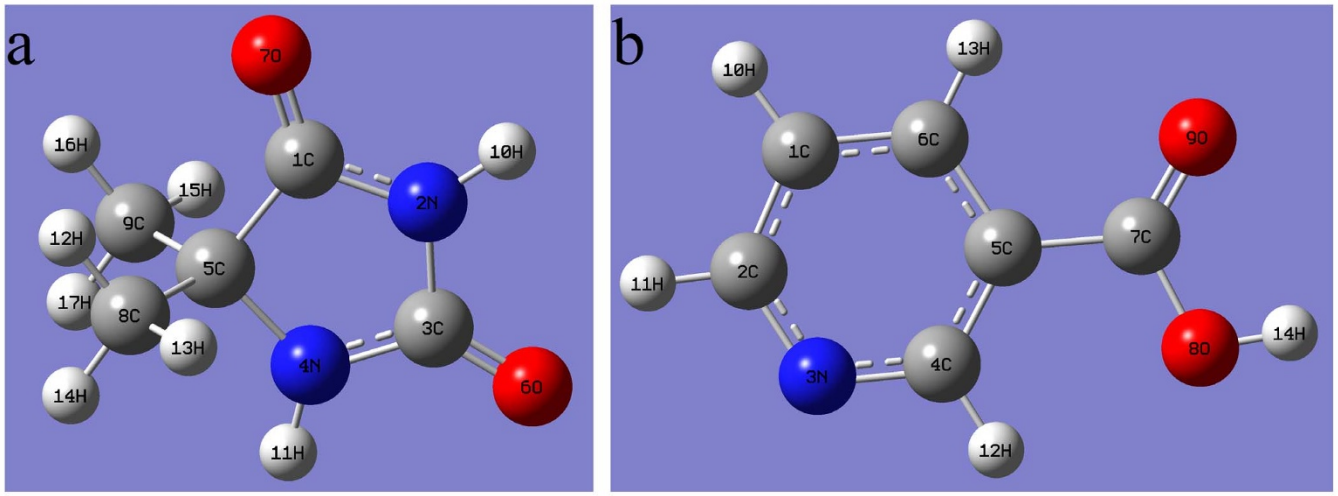

Figure 1 | **Molecular structures of (a) DMH and (b) NA.**

DFT has become a generally useful technique to study the bonding interactions between ions and complexing agents in complexes[44–48]. In this work, DFT calculations were employed to investigate the bonding interactions of complexing agents with Ag^+ in the silver electroplating bath. Another useful method is the molecular dynamic (MD) simulation, which is a convenient way to study the interactions between molecules and interfaces[35,49–54] or other questions in chemistry[55–62]. Adsorption interactions exist between complexing agents and the cathode surface during the electroplating process, which could be simulated by means of MD simulations.

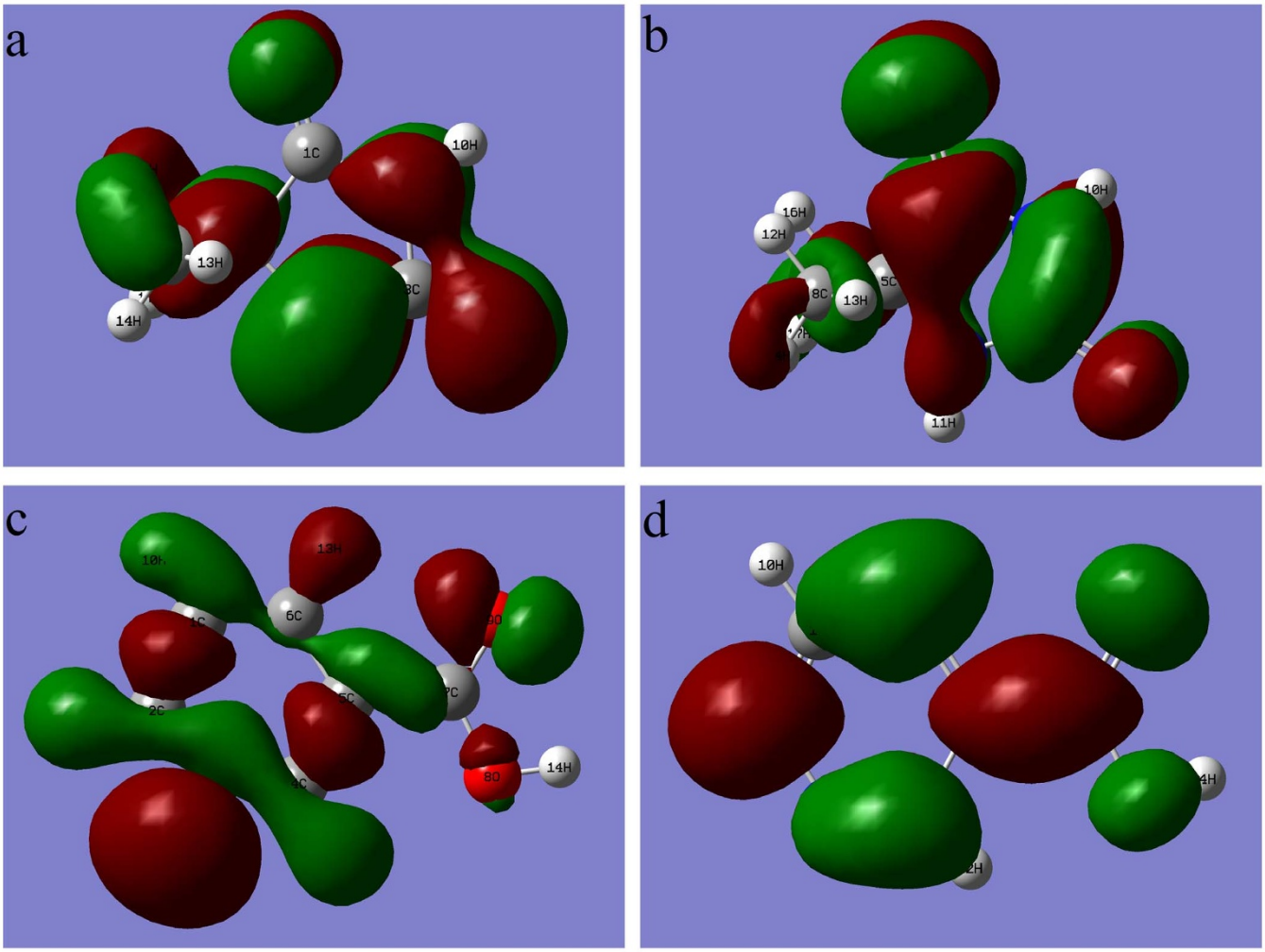

Figure 2 | **Localization of the highest occupied molecular orbital (HOMO) of (a) DMH and (c) NA, the lowest unoccupied molecular orbital (LUMO) of (b) DMH and (d) NA.**

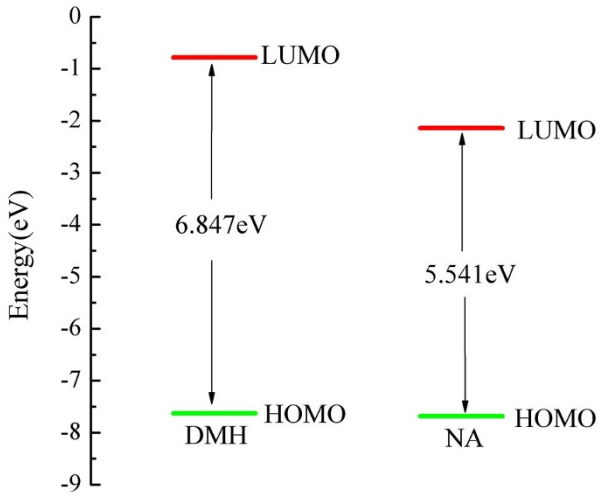

Figure 3 | Schematic diagrams of frontier molecular orbitals of DMH and NA, and the calculated E (eV).

In the present paper, 5,5-dimethylhydantoin (DMH) and nicotinic acid (NA) were selected as complexing agents for silver electroplating. DFT calculations were used to investigate the bonding interactions between complexing agents and Ag^+, and MD simulations were employed to discuss the adsorption interactions between 5,5-dimethylhydantoin (DMH), nicotinic acid (NA) and the copper, silver surface. Basing on the quantum chemical calculations and MD simulations, a synergistic effect between DMH and NA in the silver plating bath was predicted, which was further confirmed through electrochemical measurements and silver electroplating.

Results and discussion

Molecular structures and quantum chemical calculations. DMH and NA were predicted to be complexing agents for silver electroplating in this research, the molecular structures of DMH and NA were shown in Figure 1.

It can be seen both DMH and NA were heterocyclic structure organic molecules. The oxygen and nitrogen containing in such structures ensure a firmly coordination with metal ions (Ag^+) as well as the adsorption to the metal surfaces (Cu or Ag).

Quantum chemical calculations were employed to study the electronic properties, orbital information and single point energies of each agent and their silver(I)-complexes. According to the frontier molecular orbital theory, the energy of highest occupied molecular orbital (HOMO) and lowest unoccupied molecular orbital (LUMO) are often associated with the electron donating ability and electron accepting ability. The higher value of E_{HOMO} and the lower value of E_{LUMO} indicate a tendency of the molecule to donate and accept electrons, respectively. Except for the localization of MO, E_{HOMO}, E_{LUMO}, and ΔE are useful tools to characterize the electronic properties of each agent. The localization of HOMO and LUMO of DMH and NA were shown in Figure 2.

Figure 2(a) exhibited the distribution of HOMO in DMH. The carbon and oxygen atoms in DMH showed significant contribution to the HOMO, however, the 8O atom of NA did not show a significant contribution to the HOMO as shown in Figure 2(c). The contribution to the HOMO of the atoms was connected to the electron donating ability i.e. the ability of forming silver(I)-complexes coordinate bonds. Hence, as shown in Figure 2, 2N, 4N, 6O, 7O of DMH and 3N, 9O of NA could be the possible atoms forming coordinate bonds with Ag^+.

The schematic diagrams of E_{DMH} and E_{NA} based on frontier molecular orbitals were presented in Figure 3.

As shown in Figure 3, E_{HOMO} of DMH and NA were −7.630 eV and −7.680 eV, respectively. It indicated that the electron donating ability of DMH was similar to that of NA. Therefore, both DMH and NA could donate electrons to Ag^+ to form coordinate bonds with similar ability. The difference of frontier molecular orbitals in DMH and NA was mainly in LUMO, E_{LUMO} of DMH and NA were −0.783 eV and −2.139 eV, respectively. ΔE_{DMH} was 6.847 eV, whereas ΔE_{NA} was 5.541 eV. The different value of ΔE may correspond to the different stabilities of the agent-adsorption layers on the metal surface[63–65].

Based on the frontier molecular orbital calculations combined with other advantages, such as environmental compatibility, low cost, good solubility, and superior stability in alkaline solution within a large temperature range, these two organic molecules could be adopted as complexing agents for silver electroplating.

Charge distributions and structures of silver(I)-complexes. To investigate the ability of forming silver(I)-complexes coordinate bonds, quantum chemical calculations were employed to study the charge distributions of these two organic molecules, the possible structures of the silver(I)-complexes and the single point energies of the silver(I)-complexes. The charge distributions of DMH and NA were shown in Figure 4.

As the charge distributions shown in Figure 4, 2N (−0.307), 4N (−0.218), 6O (−0.474), 7O (−0.397) of DMH and 3N (−0.118), 8O (−0.207), 9O (−0.357) of NA could be the possible atoms forming coordinate bonds with Ag^+. Figure 5 presented 16 possible structures of the silver(I)-complexes with DMH and NA based on their electronic properties showed in Figure 2 and Figure 4.

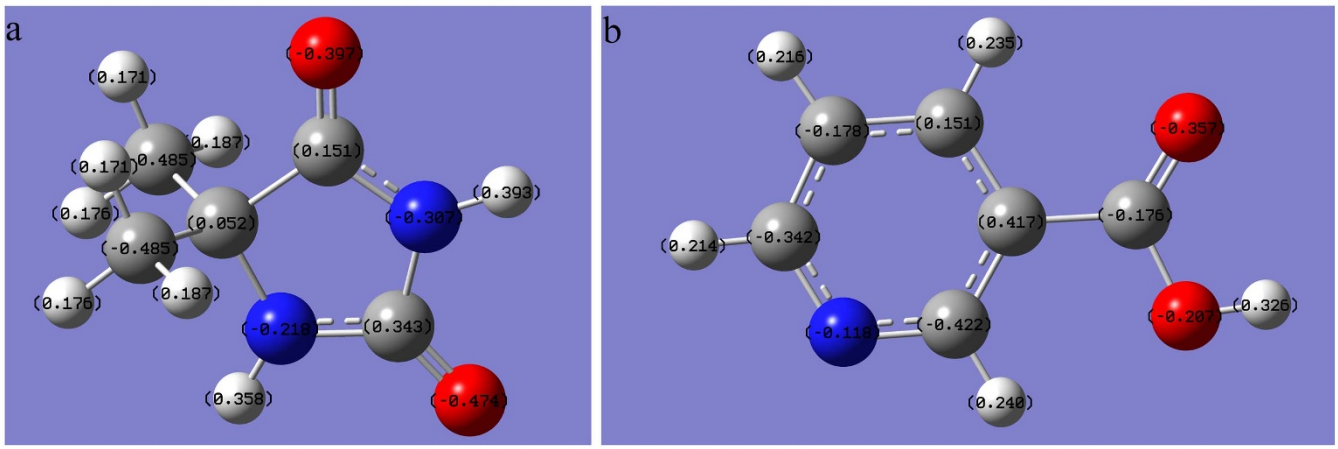

Figure 4 | Charge distributions of (a) DMH and (b) NA (unit of e).

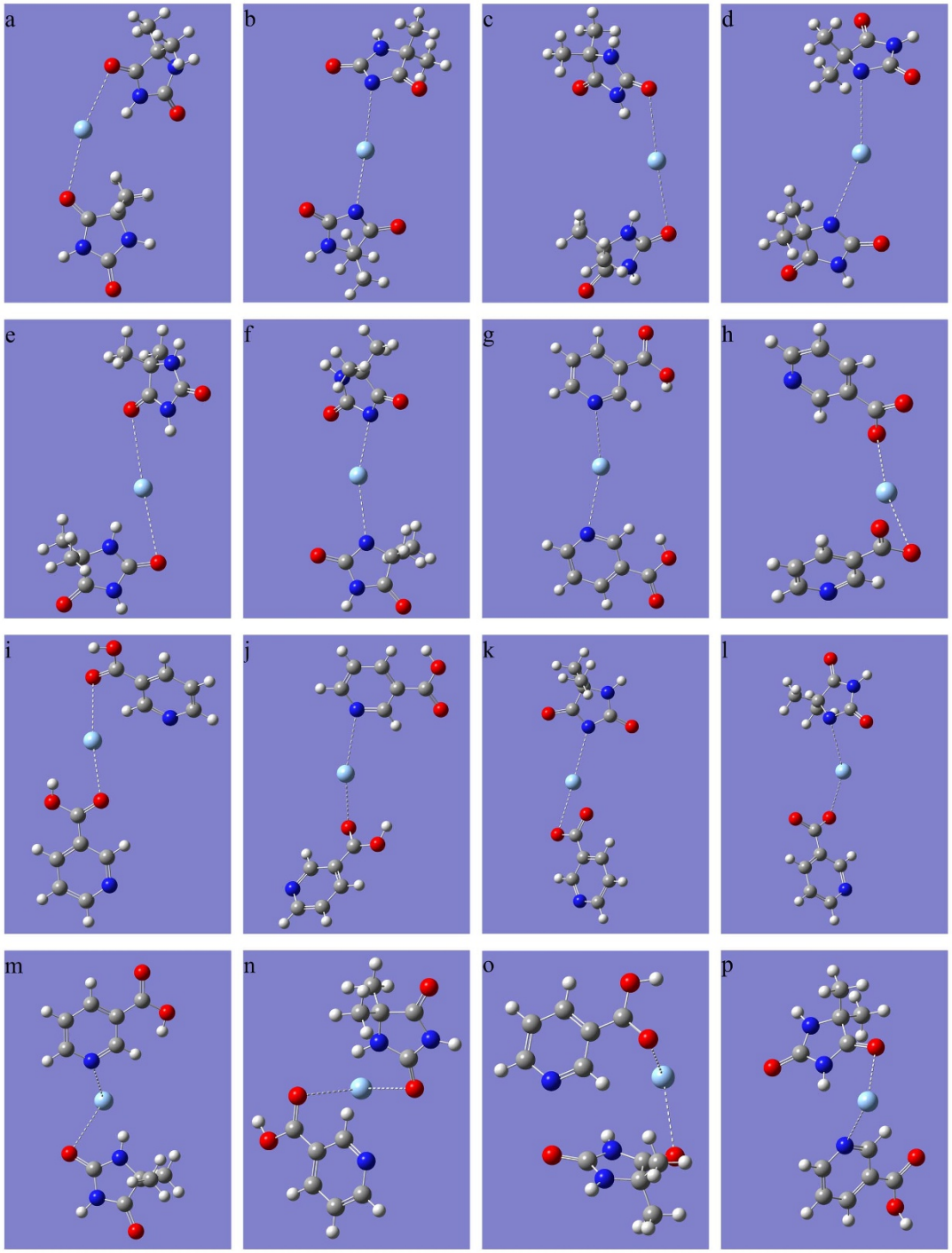

Figure 5 | Possible structures of the silver(I)-complexes with DMH and NA.

DFT calculations were performed to validate whether these 16 possible structures of the silver(I)-complexes were reasonable and stable existing in the plating bath. The final energies of different silver(I)-complexes under study were calculated at B3LYP/GENECP level and B3LYP/GENECP optimized geometries. The optimized structures of possible silver(I)-complexes were displayed in Figure 6. The key geometric parameters and bonding energies of the studied complexes were summarized in Table 1.

The main conclusions from Figure 6 and Table 1 were as follows, structure (b) (2N-Ag-2N), (d) (4N-Ag-4N), and (f) (2N-Ag-4N) of DMH-Ag-DMH, structure (h) (8O-Ag-8O) of NA-Ag-NA, structure (k) (2N-Ag-8O) and (l) (4N-Ag-8O) of DMH-Ag-NA with bonding energy −247.613 kJ/mol, −288.993 kJ/mol, −267.939 kJ/mol, −216.135 kJ/mol, −231.05 kJ/mol, and −251.927 kJ/mol, respectively, were the most possible and stable structures in the plating bath introduced in this paper. As the bonding energies shown in Table 1, the silver(I)-complexes of DMH-Ag-DMH possess high bonding energies than those of silver(I)-complexes of DMH-Ag-NA and NA-Ag-NA, demonstrating that silver(I)-complexes of DMH-Ag-DMH possess high stability in the plating bath.

Results of molecular orbital characteristic, charge distributions, geometry optimization, single point energy, and bonding energy calculations suggested that these two organic molecules could be used as complexing agents for silver electroplating. Additionally, DMH could form more strong silver(I)-complexes coordinate bonds with Ag^+ compared with NA, indicating a higher efficiency

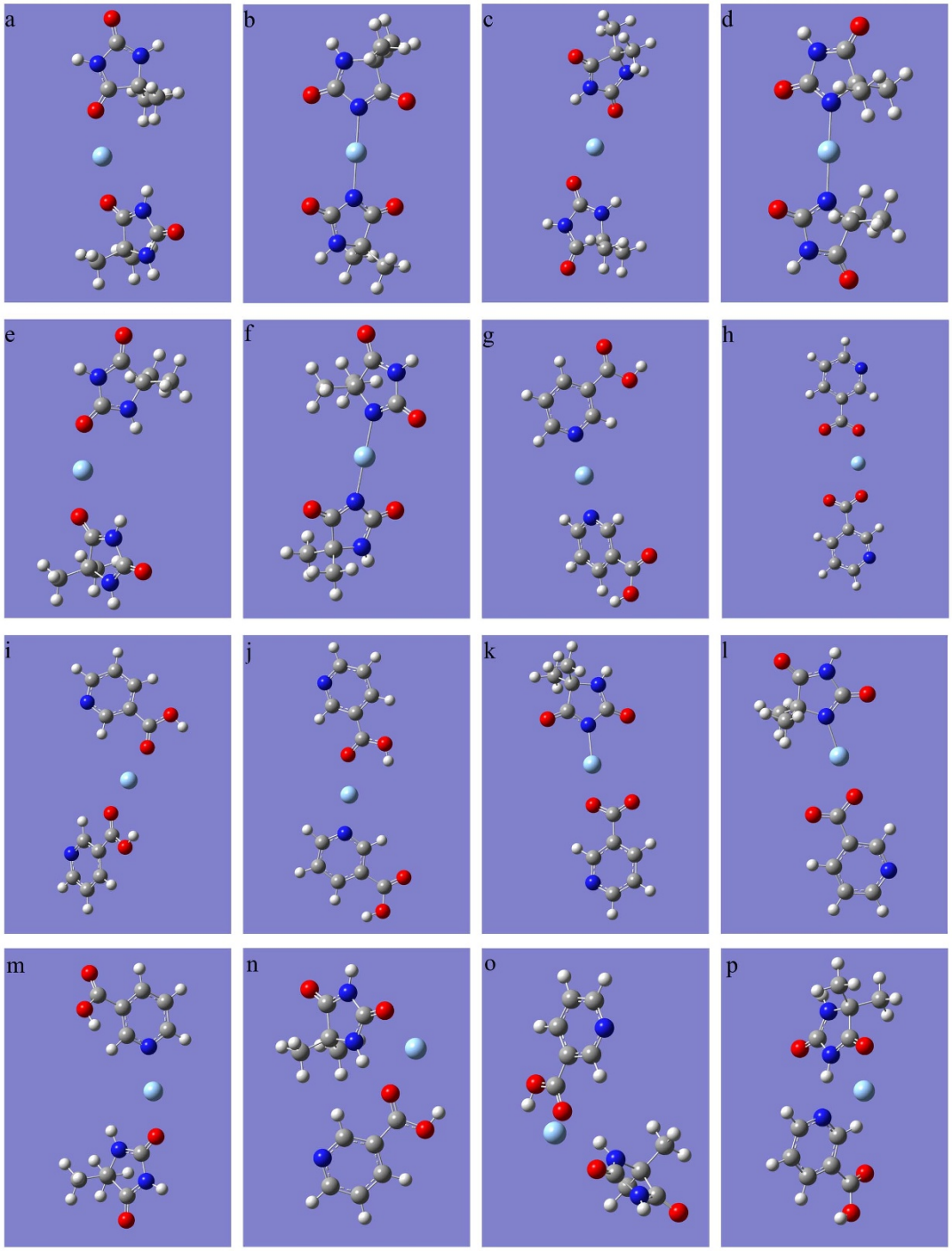

Figure 6 | Optimized structures of the silver(I)-complexes with DMH and NA.

as a complexing agent to chelate free Ag^+ in the silver electroplating bath.

Adsorption behaviors of agents on cathode surface. MD simulations were performed to study the adsorption behaviors of DMH and NA on the Cu (111) and Ag (111) surfaces. Figure 7 showed the final equilibrium configuration of the MD simulation boxes at 328 K with a time step of 1 fs and simulation time of 500 ps.

The final equilibrium configuration of the simulation boxes of DMH on Cu (111) and Ag (111) were presented in Figure 7(a) and (c), respectively. $E_{Adsorption}$ calculated from Figure 7(a) and (c) was 290.752 and 200.540 kJ/mol, respectively. Figure 7(b) and (d) displayed the final equilibrium configuration of the simulation boxes of NA on Cu (111) and Ag (111), respectively. $E_{Adsorption}$ calculated from Figure 7(b) and (d) was 338.437 kJ/mol and 252.524 kJ/mol, respectively. Moreover, as shown in Figure 7(b) and (d), the NA ring was approximately parallel to the copper and silver surface, suggesting an effective adsorption on the metal surfaces. Results of MD simulations manifested that NA could adsorb on the copper and silver surfaces more strongly than DMH, leading to a higher inhibited effect for silver electrodepositing on the copper and silver surfaces.

Basing on the conclusions of quantum chemical calculations and MD simulations, we predicted that there would be a synergistic effect between DMH and NA when jointly used as complexing agents in the silver plating bath. Electrochemical measurements and silver electroplating were carried out to further confirm the prediction.

Table 1 | Energetic data calculated with B3LYP for the complexes under study (unit of kJ/mol)

	Charge	Ag^+	DMH	NA	H_2O	H_3O^+	complexes	$E_{Bonding}$
		−382352.461	−1195927.711	−1147334.215	−200762.737	−201783.322		
a	1	1	2	0	0	0	−2774268.609	60.726
b	−1	1	2	0	2	2	−2771919.1	−247.613
c	1	1	2	0	0	0	−2774278.330	70.447
d	−1	1	2	0	2	2	−2771877.720	−288.993
e	1	1	2	0	0	0	−2774275.616	67.733
f	−1	1	2	0	2	2	−2771898.774	−267.939
g	1	1	0	2	0	0	−2677128.051	107.160
h	−1	1	0	2	2	2	−2674763.586	−216.135
i	1	1	0	2	0	0	−2677068.356	47.465
j	1	1	0	2	0	0	−2677090.473	69.582
k	−1	1	1	1	2	2	−2723342.167	−231.05
l	−1	1	1	1	2	2	−2723321.290	−251.927
m	1	1	1	1	0	0	−2725692.618	78.231
n	1	1	1	1	0	0	−2725666.917	52.53
o	1	1	1	1	0	0	−2725663.569	49.182
p	1	1	1	1	0	0	−2725650.003	35.616

Electrochemical measurements. The cathodic polarization curves measurements were employed to investigate the influences of DMH and NA on electrochemical behaviors in the silver plating baths. Figure 8 displayed the cathodic polarization curves of bath (r) containing 0.7 M DMH and 0.7 M NA, bath (s) containing 1.4 M DMH and bath (t) containing 1.4 M NA, measured by linear sweep voltammetry on a glassy carbon electrode (GCE) at a scan rate of 1 mV/s. The other contents in these three baths were $AgNO_3$ and K_2CO_3 with the same concentrations.

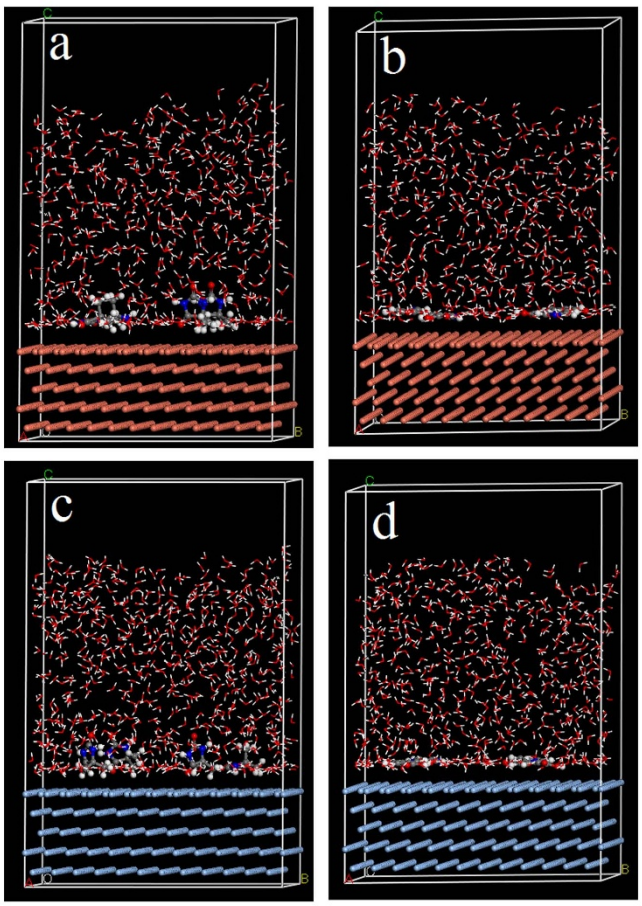

Figure 7 | The final equilibrium configuration of the MD simulation boxes, adsorption behaviors of (a) DMH and (b) NA on the Cu (111) surface, (c) DMH and (d) NA on the Ag (111) surface.

As shown in Figure 8, there were three waves of different silver plating baths. The suitable range for silver electroplating in bath (r) was about −0.5 to −1.2 V *vs* Hg/HgO, compared to −0.5 to −1.1 V for bath (s) and −0.5 to −0.9 V for bath (t). It is clearly can been seen the cathodic polarization was significantly improved by mixing DMH and NA as composite complexing agents in one bath, indicating the highest cathodic polarization of the silver(I)-complexes in bath (r). The combination of DMH and NA as composite complexing agents in one silver plating bath caused an increase in cathodic polarization, consisting well with the conclusions of quantum chemical calculations and molecular dynamic simulations.

Function of DMH and NA in silver electroplating. In the silver electroplating experiments, mirror bright silver deposits were obtained from the bath containing 0.7 M DMH and 0.7 M NA as composite complexing agents. While, in the controlled experiments, white silver deposits were originated from baths containing 1.4 M DMH or 1.4 M NA as single complexing agent at the same electroplating conditions.

The typical plating results were shown in Figure 9 and Figure 10. Figure 9 exhibited the SEM images of the top views of silver deposits obtained from different baths.

As revealed in Figure 9(a), 9(c), and 9(e), the deposit of plating bath (r) was smooth and compact, while for both bath (s) and (t), the

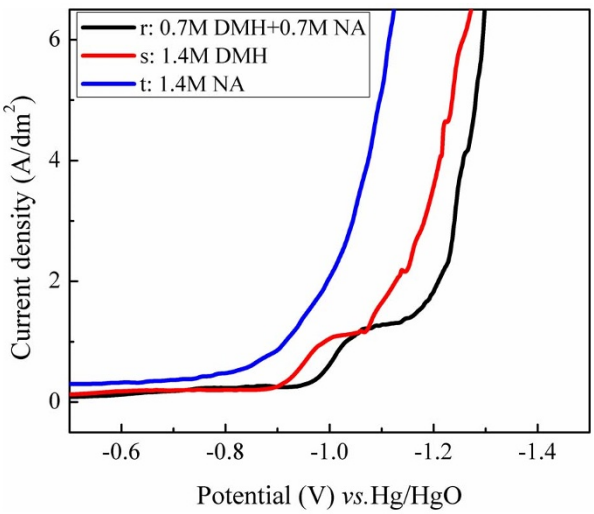

Figure 8 | Cathodic polarization curves measured by linear sweep voltammetry in three silver electroplating baths.

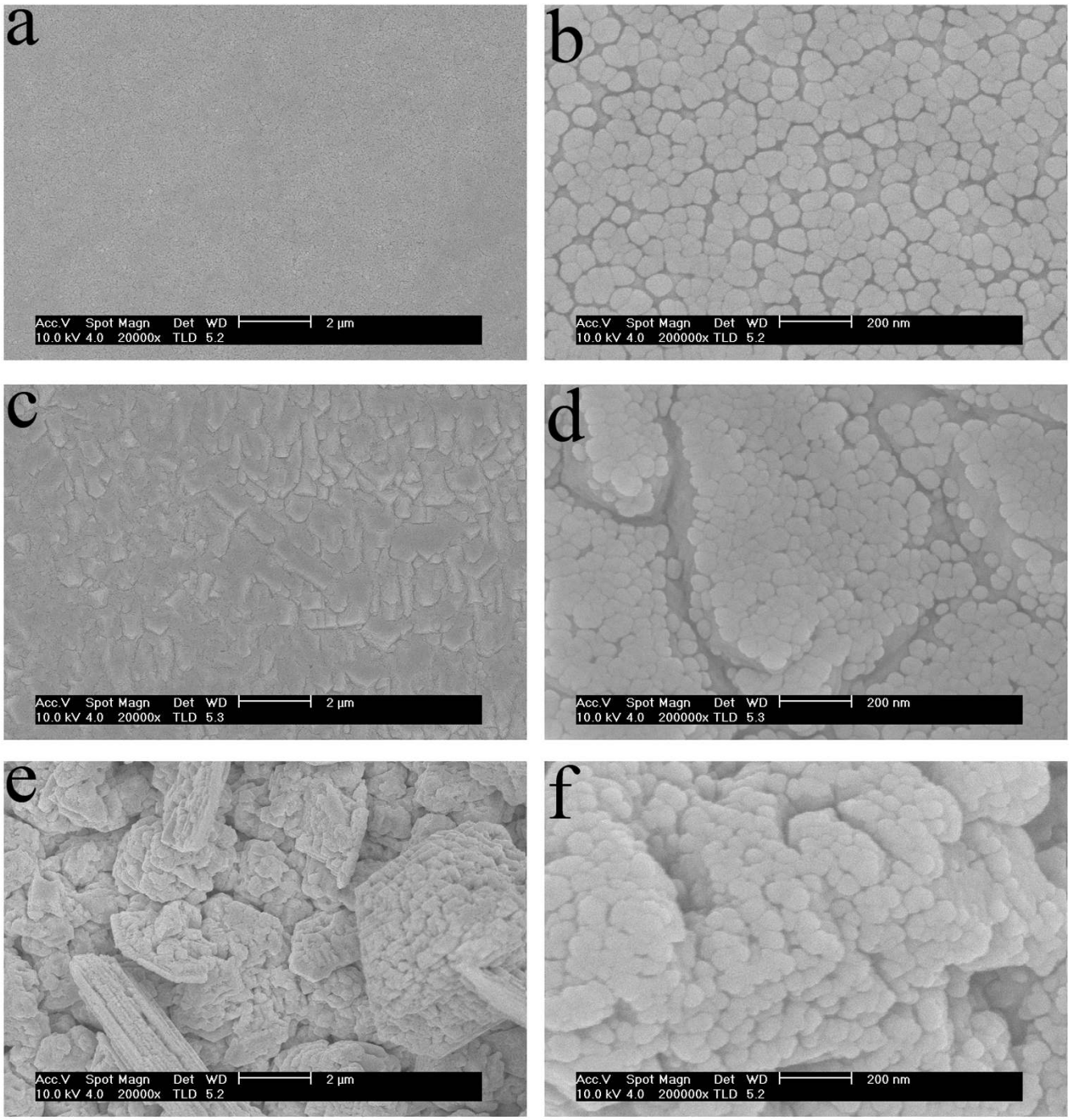

Figure 9 | SEM images of the top view of silver deposits obtained from different silver plating baths, (a) and (b) from bath (r), (c) and (d) from bath (s), (e) and (f) from bath (t).

deposits layers were much rougher Figure 9(b), 9(d), and 9(f) showed that the crystal grains of deposit obtained from plating bath (r) were smaller than that from the other two baths. In bath (s) or (t), a white and non-compact silver deposit was obtained, the particles were larger in size than those from bath (r). When using the silver plating bath containing 0.7 M DMH and 0.7 M NA as the composite complexing agents, a mirror bright and compact silver deposit was obtained with the corresponding crystal grain size decreased to less than 100 nm (as shown in Figure 9(b)). Indicating that, the combination of DMH and NA as composite complexing agents caused an increase in cathodic polarization and resulted in smaller grains in the silver deposit. Meanwhile, the deposit from bath (t) was rougher than that from bath (s) in consistent with the results of quantum chemical calculations: DMH could form silver(I)-complexes coordinate bonds with Ag^+ more strongly than NA.

AFM three-dimensional height images of the copper surface before and after silver deposits were presented in Figure 10. Checked by NanoScope Analysis, the *Ra* (*Rq*) in Figure 10 (a)–(d) was displayed in table 2.

As shown in Figure 10(a), there were some trenches on the pure copper surface. Compared to the copper surface, the silver deposit surface in Figure 10(b) showed a smoother morphology. The trenches were not existed after the copper surface was electrodeposited with silver.

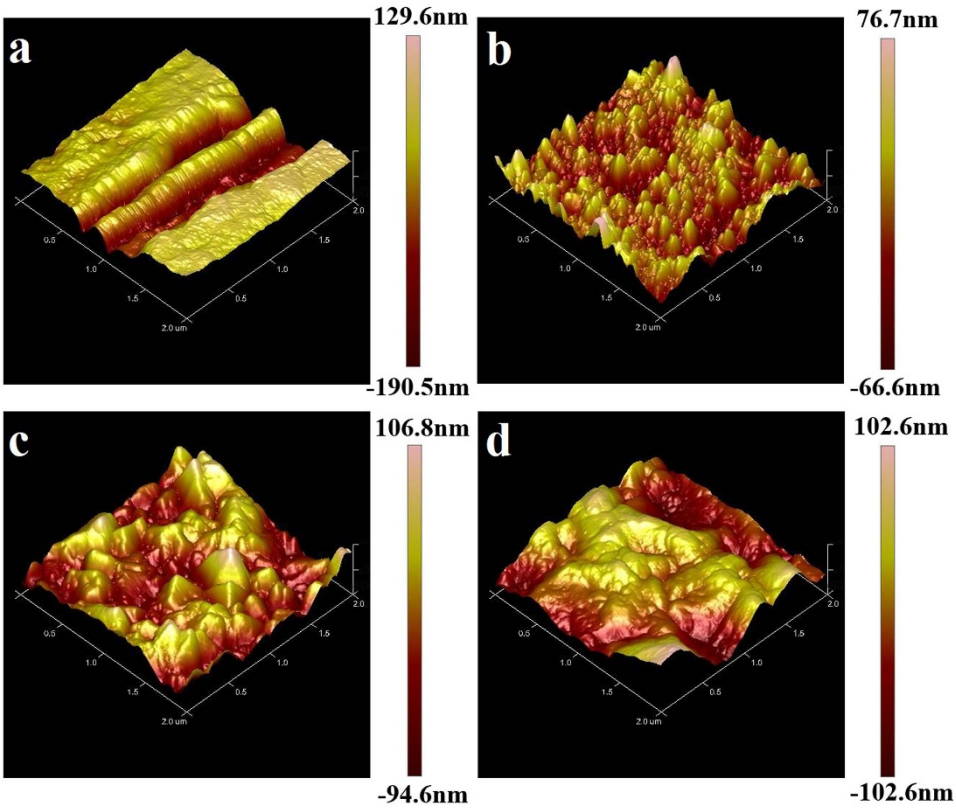

Figure 10 | **AFM three-dimensional height image of the top view of (a) the polished copper surface, deposits (b) from bath (r), (c) from bath (s), (d) from bath (t).**

From the results of AFM three-dimensional height tests of the silver deposits and the copper surface, it can be confirmed that the silver plating bath containing DMH and NA as composite complexing agents possessed excellent leveling capacity.

In conclusion of the silver electroplating, SEM and AFM tests, the silver plating bath containing DMH and NA as composite complexing agents possessed excellent bath and deposit performances. Silver(I)-complexes in this bath exhibited good complex stability, mirror bright silver deposit with excellent leveling capability, smooth, and compact morphologies could be obtained from the bath. Results of silver electroplating corroborated the conclusions of quantum chemical calculations, MD simulations, and the electrochemical measurements.

Conclusions

In summary, we reported a novel method for predicting the behavior of complexing agents in mirror bright silver electroplating using quantum chemical calculations and molecular dynamic simulations. The results of quantum chemical calculations suggested that DMH and NA could be used as potential composite complexing agents for silver electroplating based on their electronic properties and orbital information. The DFT calculations confirmed that DMH was more effective in chelating free Ag^+ in the plating bath than NA. However, NA was more effective for inhibiting silver electrodeposit on the copper and silver surfaces than DMH. In a word of the results of quantum chemical calculations and MD simulations, a synergistic effect between DMH and NA as composite complexing agents in the silver plating bath was predicted.

The electrochemical measurements showed that the combination of DMH and NA as complexing agents to one bath caused an increase in cathodic polarization, corroborating the conclusions of quantum chemical calculations and MD simulations. The SEM results showed that a compact silver deposit with the corresponding size less than 100 nm can be obtained from DMH/NA complexing agents, indicating that the combination of DMH and NA as composite complexing agents to the bath caused an increase in cathodic polarization and resulted in smaller grains in the silver deposit. From the results of AFM tests of the silver deposits and the copper surface, the silver plating bath containing DMH and NA as complexing agents possessed excellent leveling capacity.

Basing on our research, quantum chemical calculations and MD simulations could be used effectively for the prediction of complexing agents in silver electroplating. The method introduced in this paper may be easily transferred to other metal electroplating. This efficient and versatile method thus opens a new window to study or design complexing agents for generalized metal electroplating and will vigorously promote the level of this research region.

Table 2 | *Ra (Rq)* in Figs. 10(a)–(d). (unit of nm)

	10 (a)	10 (b)	10 (c)	10 (d)
Ra	45.0	15.9	25.0	28.8
Rq	54.7	20.0	30.6	35.1

Methods

Quantum chemical calculations. All quantum chemical calculations were carried out by DFT using the B3LYP functional method. In the geometry optimization, single point energy calculation, and molecular orbital characteristic analysis, 6-311++G** basis set was used for hydrogen, oxygen, carbon, and nitrogen atoms of the studied systems, respectively, except silver ions with LANL2DZ ECP basis set. All calculations on these systems under investigation were performed using Gaussian 09 program package at 328 K with solvent = water.

The bonding energy between Ag^+ and the complexing agents was calculated as equation (1).

$$E_{Bonding} = E_{Ag^+} + E_{Agents} - E_{H^+} - E_{Complexes} \quad (1)$$

$E_{Complexes}$ was the total energy of the complexes containing Ag^+ and complexing agents, E_{Ag^+}, E_{Agents} and E_{H^+} (E_{H3O^+}) was the total energy of the free Ag^+, agents, and H^+ (H_3O^+), respectively.

Molecular dynamic simulations. Molecular dynamic (MD) simulations of the adsorption interactions between DMH, NA and the copper, silver surfaces were carried out in a simulation box with periodic boundary conditions using Materials Studio (from Accelrys Inc). The box consisted of a silver or copper surface (cleaved along the (111) plane), a liquid phase, and a vacuum layer of 1 nm height. The liquid phase contained water molecules with density of 1 g/cm^3 and four DMH or NA molecules.

The MD simulations were performed at 328 K, NVT ensemble and COMPASS forcefield, with a time step of 1 fs and simulation time of 500 ps. The interaction energy between the metal surface and organic molecules was calculated as equation (2).

$$E_{Interaction} = E_{Total} - E_{Metal} - E_{Agents} \quad (2)$$

E_{Total} was the total energy of the copper or silver crystal together with the adsorbed complexing agents, E_{Metal} and E_{Agents} were the total energy of the copper or silver crystal and free agents, respectively. The adsorption energy was the negative value of the interaction energy, $E_{Adsorption} = -E_{Interaction}$.

Electrochemical measurements and silver electroplating. All solutions were of analytical grade reagents and deionized water was utilized throughout this work. The silver plating bath was prepared by adding $AgNO_3$ solution into a solution containing DMH, NA, and K_2CO_3, the pH value of the bath was adjusted to 10.0 ~ 14.0 with KOH solution.

All of the electrochemical measurements were performed in a three-electrode cell using a potentiostat/galvanostat (PARSTAT2273 Electrochemical Integrated Test System, Princeton Applied Research) at 328 K. A glassy carbon electrode (GCE) with a diameter of 3 mm was employed as the working electrode (WE). The counter electrode (CE) was a platinum plate with an area of 1 cm^2. A mercuric oxide electrode (Hg/HgO) was used as the reference electrode (RE). Silver electroplating experiments were conducted under galvanostatic conditions, a cell with a silver anode and a copper substrate was employed.

Field emission scanning electron microscopy (FESEM, FEI XL30S-FEG) was used to study the surface morphologies of the silver deposits. Atomic force microscope (AFM) was employed to study the surface roughness of the silver deposits. The AFM analysis was carried out with a Dimension Icon (Bruker), working in contact mode with silicon nitride cantilevers.

1. Blair, A. Silver plating. *Met. Finish.* **97**, 303–308 (1999).
2. Marquez, K., Staikov, G. & Schultze, J. W. Silver deposition on silicon and glassy carbon. A comparative study in cyanide medium. *Electrochim. Acta* **48**, 875–882 (2003).
3. Baker, B. C. *et al.* Superconformal electrodeposition of silver from a KAg(CN)2-KCN-KSeCN electrolyte. *J. Electrochem. Soc.* **150**, C61–C66 (2003).
4. Bozzini, B., D'Urzo, L., Mele, C. & Romanello, V. A SERS investigation of cyanide adsorption and reactivity during the electrodeposition of gold, silver, and copper from aqueous cyanocomplexes solutions. *J. Phys. Chem. C.* **112**, 6352–6358 (2008).
5. Hossain, S. M. A. & Saitou, M. Surface roughness of thin silver films pulse-plated using silver cyanide-thiocyanate electrolyte. *J. Appl. Electrochem.* **38**, 1653–1657 (2008).
6. Baltrunas, G. The mechanism of electrode process in the system silver/silver cyanide complexes. *Electrochim. Acta* **48**, 3659–3664 (2003).
7. Chen, J. S. *et al.* Electrodeposition of bright gold-a green path using hypoxanthine as a complexing agent. *Green Chem.* **13**, 2339–2343 (2011).
8. Leahy, E. P. & Karustis, G. A. Non-cyanide acidic silver electroplating bath and additive therefore. *US Pat.* 4067784 (1978).
9. Nobel, F. I., Brasch, W. R. & Drago, A. J. Cyanide-free plating solutions for monovalent metals. *US Pat.* 5302278 (1994).
10. Asakawa, T. Silver plating baths and silver plating method using the same. *US Pat.* 5601696 (1997).
11. Morrissey, R. J. Non-cyanide silver plating bath composition. *US Pat.* 20070151863 (2007).
12. Clauss, M. & Zhang-Berlinger, W. Cyanide-free silver electroplating solutions. *US Pat.* 20120067735 (2012).
13. Xie, B. G., Sun, J. J., Lin, Z. B. & Chen, G. N. Electrodeposition of Mirror-Bright Silver in Cyanide-Free Bath Containing Uracil as Complexing Agent Without a Separate Strike Plating Process. *J. Electrochem. Soc.* **156**, D79–D83 (2009).
14. Hradil, E., Hradil, H. & Weisberg, A. M. Silver complex, method of making said complex and method and electrolyte containing said complex for electroplating silver and silver alloys. *US Pat.* 4126524 (1978).
15. Hradil, E., Hradil, H. & Weisberg, A. M. Non-cyanide bright silver electroplating bath therefor, silver compounds and method of making silver compounds. *US Pat.* 4246077 (1981).
16. Valiuniene, A., Baltrunas, G., Valiunas, R. & Popkirov, G. Investigation of the electroreduction of silver sulfite complexes by means of electrochemical FFT impedance spectroscopy. *J. Hazard. Mater.* **180**, 259–263 (2010).
17. Hernandez, M. M. & Gonzalez, I. Effect of Potential on the Early Stages of Nucleation and Growth during Silver Electrocrystallization in Ammonium Medium on Vitreous Carbon. *J. Electrochem. Soc.* **151**, C220–C228 (2004).
18. Polk, B. J., Bernard, M., Kasianowicz, J. J., Misakian, M. & Gaitan, M. Microelectroplating Silver on Sharp Edges toward the Fabrication of Solid-State Nanopores. *J. Electrochem. Soc.* **151**, C559–C566 (2004).
19. Pardavé, M. P., Ramírez, M. T., González, I., Serruya, A. & Scharifker, B. R. Silver Electrocrystallization on Vitreous Carbon from Ammonium Hydroxide Solutions. *J. Electrochem. Soc.* **143**, 1551–1558 (1996).
20. Reents, B., Plieth, W., Macagno, V. A. & Lacconi, G. I. Influence of thiourea on silver deposition: Spectroscopic investigation. *J. Electroanal. Chem.* **453**, 121–127 (1998).
21. Azzaroni, O., Schilardi, P. L., Salvarezza, R. C. & Arvia, A. J. Smoothening Mechanism of Thiourea on Silver Electrodeposition. Real Time Imaging of the Growth Front Evolution. *Langmuir.* **15**, 1508–1514 (1999).
22. de Oliveira, G. M., Silva, M. R. & Carlos, I. A. Voltammetric and chronoamperometric studies of silver electrodeposition from a bath containing HEDTA. *J. Mater. Sci.* **42**, 10164–10172 (2007).
23. Lin, Z. B., Xie, B. G., Chen, J. S., Sun, J. J. & Chen, G. N. Nucleation mechanism of silver during electrodeposition on a glassy carbon electrode from a cyanide-free bath with 2-hydroxypyridine as a complexing agent. *J. Electroanal. Chem.* **633**, 207–211 (2009).
24. Lin, Z. B. *et al.* Electrochemical and in Situ SERS Studies on the Adsorption of 2-Hydroxypyridine and Polyethyleneimine during Silver Electroplating. *J. Phys. Chem. C* **113**, 9224–9229 (2009).
25. Basile, A., Bhatt, A. I., O'Mullane, A. P. & Bhargava, S. K. An investigation of silver electrodeposition from ionic liquids: Influence of atmospheric water uptake on the silver electrodeposition mechanism and film morphology. *Electrochim. Acta* **56**, 2895–2905 (2011).
26. Yeh, F. H., Tai, C. C., Huang, J. F. & Sun, I. W. Formation of porous silver by electrochemical alloying/dealloying in a water-insensitive Zinc Chloride-1-ethyl-3-methyl Imidazolium Chloride Ionic Liquid. *J. Phys. Chem. B.* **110**, 5215–5222 (2006).
27. Tsai, M. C., Zhuang, D. X. & Chen, P. Y. Electrodeposition of macroporous silver films from ionic liquids and assessment of these films in the electrocatalytic reduction of nitrate. *Electrochim. Acta* **55**, 1019–1027 (2010).
28. Bomparola, R., Caporali, S., Lavacchi, A. & Bardi, U. Silver electrodeposition from air and water-stable ionic liquid: An environmentally friendly alternative to cyanide baths. *Surf. Coat. Technol.* **201**, 9485–9490 (2007).
29. Lanyon, B. P. *et al.* Towards quantum chemistry on a quantum computer. *Nature Chem.* **2**, 106–111 (2010).
30. Zimmerman, P. M., Zhang, Z. Y. & Musgrave, C. B. Singlet fission in pentacene through multi-exciton quantum states. *Nature Chem.* **2**, 648–652 (2010).
31. Kurashige, Y., Chan, G. K. L. & Yanai, T. Entangled quantum electronic wavefunctions of the Mn_4CaO_5 cluster in photosystem II. *Nature Chem.* **5**, 660–666 (2013).
32. Perczel, A., Hudáky, P. & Pálfi, V. Dead-End Street of Protein Folding: Thermodynamic Rationale of Amyloid Fibril Formation. *J. Am. Chem. Soc.* **129**, 14959–14965 (2007).
33. Truhlar, D. G. Inverse solvent design. *Nature Chem. advance online publication* 1–2 (2013).
34. Bickerton, G. R., Paolini, G. V., Besnard, J., Muresan, S. & Hopkins, A. L. Quantifying the chemical beauty of drugs. *Nature Chem.* **4**, 90–98 (2012).
35. Lopez-Acevedo, O., Kacprzak, K. A., Akola, J. & Häkkinen, H. Quantum size effects in ambient CO oxidation catalysed by ligand-protected gold clusters. *Nature Chem.* **2**, 329–334 (2010).
36. Huang, M. *et al.* Dissecting the mechanisms of a class of chemical glycosylation using primary ^{13}C kinetic isotope effects. *Nature Chem.* **4**, 663–667 (2012).
37. Cohen, A. J., Mori-Sanchez, P. & Yang, W. Challenges for Density Functional Theory. *Chem. Rev.* **112**, 289–320 (2012).
38. Frantzius, G. v., Ferao, A. E. & Streubel, R. Coordination of CO to low-valent phosphorus centres and other related P–C bonding situations. A theoretical case study. *Chem. Sci.* **4**, 4309–4322 (2013).
39. Geerlings, P., De Proft, F. & Langenaeker, W. Conceptual Density Functional Theory. *Chem. Rev.* **103**, 1793–1873 (2003).
40. Armstrong, D. R. *et al.* Alkali-metal-mediated zincation (AMMZn) meets N-heterocyclic carbene (NHC) chemistry: Zn–H exchange reactions and structural authentication of a dinuclear Au(I) complex with a NHC anion. *Chem. Sci.* **4**, 4259–4266 (2013).
41. Liang, Y. *et al.* Mechanism, Regioselectivity, and the Kinetics of Phosphine-Catalyzed [3 + 2] Cycloaddition Reactions of Allenoates and Electron-Deficient Alkenes. *Chem. Eur. J.* **14**, 4361–4373 (2008).
42. Yu, D. C., Yazaydin, A. O., Lane, J. R., Dietzel, P. D. C. & Snurr, R. Q. A combined experimental and quantum chemical study of CO_2 adsorption in the metal–organic framework CPO-27 with different metals. *Chem. Sci.* **4**, 3544–3556 (2013).
43. Li, K. *et al.* Light-emitting platinum(II) complexes supported by tetradentate dianionic bis(*N*-heterocyclic carbene) ligands: towards robust blue electrophosphors. *Chem. Sci.* **4**, 2630–2644 (2013).

44. Vela, J. *et al.* Bidentate Coordination of Pyrazolate in Low-Coordinate Iron(II) and Nickel(II) Complexes. *Angew. Chem. Int. Ed.* **45**, 1607–1611 (2006).
45. Cantat, T., Mezailles, N., Ricard, L., Jean, Y. & Floch, P. L. A Bis(thiophosphinoyl)methanediide Palladium Complex: Coordinated Dianion or Nucleophilic Carbene Complex? *Angew. Chem. Int. Ed.* **43**, 6382–6385 (2004).
46. Wu, J., Kan, Y. H., Wu, Y. & Su, Z. M. Computational Design of Host Materials Suitable for Green-(Deep)Blue Phosphors through Effectively Tuning the Triplet Energy While Maintaining the Ambipolar Property. *J. Phys. Chem. C.* **117**, 8420–8428 (2013).
47. Zhu, Y. L., Zhou, S. Y., Kan, Y. H. & Su, Z. M. Theoretical investigation of electronic structures and excitation energies of hexaphyrin and its group 11 transition metal (III) complexes. *J. Organomet. Chem.* **694**, 3012–3018 (2009).
48. Chan, S. L. F., Kan, Y. H., Yip, K. L., Huang, J. S. & Che, C. M. Ruthenium complexes of 1,4,7-trimethyl-1,4,7-triazacyclononane for atom and group transfer reactions. *Coord. Chem. Rev.* **255**, 899–919 (2011).
49. Gunsteren, W. F. v. & Berendsen, H. J. C. Computer Simulation of Molecular Dynamics: Methodology, Applications, and Perspectives in Chemistry. *Angew. Chem. Int. Ed. Engl.* **29**, 992–1023 (1990).
50. Hung, A. *et al.* Amphiphilic amino acids: a key to adsorbing proteins to nanopatterned surfaces? *Chem. Sci.* **4**, 928–937 (2013).
51. Düren, T., Bae, Y. S. & Snurr, R. Q. Using molecular simulation to characterise metal–organic frameworks for adsorption applications. *Chem. Soc. Rev.* **38**, 1237–1247 (2009).
52. Xia, S. W., Qiu, M., Yu, L. M., Liu, F. G. & Zhao, H. Z. Molecular dynamics and density functional theory study on relationship between structure of imidazoline derivatives and inhibition performance. *Corros. Sci.* **50**, 2021–2029 (2008).
53. Kornherr, A. *et al.* Molecular dynamics simulations of the adsorption of industrial relevant silane molecules at a zinc oxide surface. *J. Chem. Phys.* **119**, 9719–9728 (2003).
54. Kornherr, A., Hansal, S., Hansal, W. E. G., Nauer, G. E. & Zifferer, G. Molecular Dynamics Simulations of the First Steps of the Formation of Polysiloxane Layers at a Zinc Oxide Surface. *Macromol. Symp.* **217**, 295–300 (2004).
55. Speybroeck, V. v. & Meier, R. J. A recent development in computational chemistry: chemical reactions from first principles molecular dynamics simulations. *Chem. Soc. Rev.* **32**, 151–157 (2003).
56. Hong, G. Y., Ivnitski, D. M., Johnson, G. R., Atanassov, P. & Pachter, R. Design Parameters for Tuning the Type 1 Cu Multicopper Oxidase Redox Potential: Insight from a Combination of First Principles and Empirical Molecular Dynamics Simulations. *J. Am. Chem. Soc.* **133**, 4802–4809 (2011).
57. Yancey, D. F. *et al.* A theoretical and experimental examination of systematic ligand-induced disorder in Au dendrimer-encapsulated nanoparticles. *Chem. Sci.* **4**, 2912–2921 (2013).
58. LeBard, D. N., Martin, D. R., Lin, S., Woodbury, N. W. & Matyushov, D. V. Protein dynamics to optimize and control bacterial photosynthesis. *Chem. Sci.* **4**, 4127–4136 (2013).
59. Olausson, B. E. S. *et al.* Molecular Dynamics Simulations Reveal Specific Interactions of Post-translational Palmitoyl Modifications with Rhodopsin in Membranes. *J. Am. Chem. Soc.* **134**, 4324–4331 (2012).
60. Liang, S. & Kusalik, P. G. Exploring nucleation of H_2S hydrates. *Chem. Sci.* **2**, 1286–1292 (2011).
61. Wegner, M. *et al.* The impact of the amide connectivity on the assembly and dynamics of benzene-1,3,5-tricarboxamides in the solid state. *Chem. Sci.* **2**, 2040–2049 (2011).
62. Lucas, M. *et al.* Hindered rolling and friction anisotropy in supported carbon nanotubes. *Nat. Mater.* **8**, 876–881 (2009).
63. Wang, C., Zhang, J. Q., Yang, P. X. & An, M. Z. Electrochemical behaviors of Janus Green B in through-hole copper electroplating: An insight by experiment and density functional theory calculation using Safranine T as a comparison. *Electrochim. Acta.* **92**, 356–364 (2013).
64. Barouni, K. *et al.* Some amino acids as corrosion inhibitors for copper in nitric acid solution. *Mater Lett.* **62**, 3325–3327 (2008).
65. Issami, S. E. *et al.* Triazolic compounds as corrosion inhibitors for copper in hydrochloric acid. *Pigm. Resin. Technol.* **36**, 161–168 (2007).

Acknowledgments

The authors are grateful for financial support from the State Key Laboratory of Urban Water Resource and Environment (Harbin Institute of Technology) (2012DX03).

Author contributions

A.M.L., X.F.R. and B.W. carried out the experiments and performed data processing. A.M.L., X.F.R. and M.Z.A. developed the experimental set-up. A.M.L., X.F.R., M.Z.A. and C.W. designed the experiments and proposed the mechanism. J.Q.Z., P.X.Y., B.W. and Y.M.Z. reviewed the manuscript. All authors contributed to the discussion of the results as well as to the writing of the manuscript.

Additional information

Competing financial interests: The authors declare no competing financial interests.

How to cite this article: Liu, A.M. *et al.* A Combined Theoretical and Experimental Study for Silver Electroplating. *Sci. Rep.* **4**, 3837; DOI:10.1038/srep03837 (2014).